# Exploiting Polarization and Color to Enable MIMO Backscattering with Light

Seyed Keyarash Ghiasi
Delft University of Technology
Marco Zuniga
Delft University of Technology

## Abstract

Multiple-input multiple-output (MIMO) methods play a pivotal role in increasing the capacity of wireless communication systems, but they have not been analyzed systematically in the nascent area of *passive* communication with visible light (passive-VLC). The main challenge in passive-VLC is its low data rate. This limitation is caused by the slow switching speed of the most popular modulator used in the state-of-the-art: liquid crystal cells (LCs). Several studies use sophisticated modulation schemes with multiple LCs to increase the data rate. However, these efforts have only led to logarithmic improvements. A transmitter with a single LC can provide 1 kbps, and a transmitter with 64 LCs delivers 8 kbps: resulting in an efficiency of 125 bps per LC cell. Ideally, the capacity should increase linearly with the number of LCs.

We propose a *general* framework to achieve reliable MIMO communications with passive-VLC. Our approach, which has a theoretical and empirical foundation, has three desirable properties: (i) does not assume orthogonality of the individual channels (overcomes co-channel interference), (ii) can exploit multiple properties of light (polarization and color); and (iii) is agnostic to LC parameters (which some studies rely on). Our results show that a transmitter with 9 LCs *increases its capacity almost linearly up to 9 channels*, attaining 6.8 kbps (750 bps per LC) *using the simplest modulation method* in the SoA.

## CCS Concepts

• **Hardware** → *Wireless devices*; PCB design and layout; • **Networks** → Physical links.

## Keywords

Visible light communications,MIMO systems, Wireless communications, Networked Sensors

**ACM Reference Format:**
Seyed Keyarash Ghiasi, Delft University of Technology and Marco Zuniga, Delft University of Technology . 2024. Exploiting Polarization and Color to Enable MIMO Backscattering with Light. In *ACM Conference on Embedded Networked Sensor Systems (SenSys '24), November 4–7, 2024, Hangzhou, China.* ACM, New York, NY, USA, 13 pages. https://doi.org/10.1145/3666025.3699373


*SenSys '24, November 4–7, 2024, Hangzhou, China*

ACM ISBN 979-8-4007-0697-4/24/11
https://doi.org/10.1145/3666025.3699373

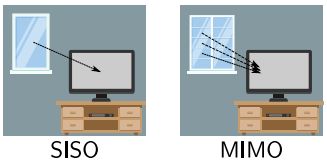


**Figure 1. MIMO for passive-VLC: we exploit polarization and color to create multiple channels.**

## 1 Introduction

Our societies are experiencing an ever-increasing demand for wireless communication, and the ubiquity of those wireless systems depends on three main components: *bandwidth*, *spatial multiplexing*, and *spectral efficiency* (more bits per Hz). Visible light communication (VLC) has been identified as a key technology for 5G as it fares well on those three metrics [5]. In VLC, standard light sources modulate their intensity to transmit information, exploiting the *broad spectrum* and *high spatial efficiency* of light bulbs. On top of that, this spectrum is unlicensed and free. Regarding *spectral efficiency*, VLC borrows methods from radio-frequency (RF) systems, such as OFDM and MIMO, which enable the design of commercial VLC products with tens of Mbps, and research platforms with several Gbps [2, 18].

Motivated by these advances, researchers are investigating *passive* VLC to enable low-power transmitters. The power consumption of a VLC transmitter depends on two main tasks: light emission and modulation. Among these tasks, light emission is the most power-hungry, requiring several watts or even tens of watts. Passive-VLC eliminates the transmitter's emission costs by modulating the light radiated by other sources. The transmitters rely on small optical modulators, such as liquid crystal cells (LCs), which consume little power and can control the intensity of light.

**Challenge:** Passive-VLC inherits the broad spectrum and high spatial efficiency of VLC, but the spectral efficiency is low. While VLC transmitters achieve speeds of Mbps and Gbps, passive platforms using LCs deliver between a few hundred bps [23] up to 8 kbps [20]. The reason for these low data rates is the slow switching speed of the optical modulators. Although some LCs can reach switching speeds in the order of tens of microseconds [16], they are expensive. Most passive transmitters rely on inexpensive LCs with switching speeds between 4 ms and 8 ms, which in turn lead to wireless carriers between 125 Hz and 250 Hz. To overcome this limitation, many studies have proposed complex platforms and modulation schemes to build links with 1 kbps, using a 125 Hz carrier; and 8 kbps using a 250 Hz carrier. However, except for a single study that proposes a novel feature space [21], MIMO has not been

Seyed Keyarash Ghiasi
Delft University of Technology and Marco Zuniga
Delft University of Technology

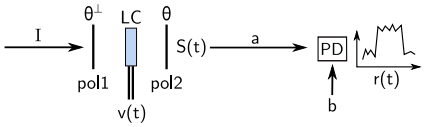


**Figure 2. The basic SISO link with two polarizers.**

the technique used to increase the data rate of passive systems. This is a missed opportunity because a unique advantage of MIMO is multiplying the capacity of a link without requiring more spectrum or faster modulators.

For passive-VLC, the use of MIMO is relevant because of the interplay between the *massive amounts of radiated light* in our environments and the *size of light modulating surfaces*. From a passive-VLC perspective, every object that reflects light (e.g. a road sign) is a potential transmitter. Considering the small size of passive-VLC antennas (in the order of millimeters), large reflective surfaces in our environments could accommodate massive amounts of antennas to increase their capacity. As shown in Figure 1, such MIMO systems could enhance applications proposed in the state-of-the-art (SoA). For example, bigger road signs could create more channels to obtain more information [19]; or the vast facade of buildings could be transformed into massive MIMO transmitters.

**Contributions:** To realize the vast potential of backscattered light for communication, we need a solid understanding of MIMO. This work provides a powerful tool that is still missing in passive-VLC: a principled MIMO approach.

*Contribution 1: A MIMO framework for passive-VLC.* In contrast to traditional RF and VLC systems, where MIMO is well-established, there is no such theoretical formulation for passive-VLC. We adapt those principles to suit the unique characteristics of LCs. Our approach has three desirable properties: (i) does not assume orthogonality of the individual channels (overcomes co-channel interference); (ii) exploits multiple properties of light (polarization and color), and (iii) is agnostic to LC parameters (which many studies rely on).

*Contribution 2: Efficient multiplexing for different light properties.* Our MIMO system can be used with color, polarization, or both; and the complexity of the channel estimation depends on how these two properties are combined. We develop *flat* and *hierarchical* schemes to optimize the channel estimation and recovery of the signals.

*Contribution 3: Design of platforms and evaluation.* We build a MIMO platform, where we show that the link capacity increases almost linearly up to a certain number of channels, even with co-channel interference. We test our mathematical approach with two types of LCs that have switching speeds comparable to other platforms. *A key strength of our mathematical framework is that it allows using the* ***simplest*** *modulation method in the SoA*, instead of using elaborated schemes. Using off-the-shelf optical elements, our system achieves a linear increase in its data rate up to 6.8 kbps, using a maximum of 9 cells.

## 2 Theoretical model

Our framework builds upon the basics of RF MIMO, and we adapt it to the particular characteristics of passive VLC. We start with a simple SISO model and then extend it to MIMO.

### 2.1 Single transmitter and receiver

To begin with the simplest case, we discuss a SISO link consisting of one transmitter and one receiver. Most SoA studies fall in this category. In these links, the transmitters usually employ LCs thanks to their simplicity and low cost. An LC cell is made of a liquid crystal layer sandwiched between two perpendicular polarizing sheets. When a voltage is applied to the LC layer, the cell turns transparent, and when there is no voltage, the cell becomes opaque, or vice versa, depending on the cell's design. We abstract this property with a transfer function $S(t)$ for the LC cell. $S(t)$ represents how much a cell attenuates the light when the voltage $v(t)$ on the LC cells changes, as shown in Figure 2. $S$ is a function of v(t), however, we denote it as $S(t)$ to facilitate the notation.

In a SISO link, the transmitted data is embedded into the optical signal $S(t)$, and the aim of the link is to recover the transmitted bits from this signal. To model how $S(t)$ looks in the receiver, we derive it by considering the effects of each LC component:

*1) Effect of the first polarizer (pol1) with angle $\theta^{\perp}$.* Following Malus' law[1], the intensity of *unpolarized* light is halved after passing through a polarizer, regardless of the polarizer's angle. In addition, the polarization of the light exiting this layer is equal to $\theta^{\perp}$. So, if the input light is unpolarized with intensity $I$, the exiting light will be $\theta^{\perp}$-polarized with intensity $0.5I$.

*2) Effect of the liquid crystal layer.* The LC layer changes the polarization of the input light as a function of the voltage $v(t)$. We model this polarization change with $\Theta(v(t))$. In off-the-shelf cells, the range of $\Theta(v(t))$ is [0°,90°]. After the LC layer, the polarization angle of the light is $\theta^{\perp} + \Theta(v(t))$. In a SISO link, the transmitter modulates $v(t)$, which in turn, modulates the light's polarization. Keeping this in mind, we omit $v(.)$ from our notation and use $\Theta(t)$ for brevity.

*3) Effect of the second polarizer (pol2): $\theta = \theta^{\perp} - 90°$.* This polarizer is placed after the LC layer, and is perpendicular to the first polarizer. Malus' law states that the light undergoes an attenuation of $\cos^2(\theta^{\perp} + \Theta(t) - \theta)$ after crossing the second polarizer. Also, $\theta^{\perp} - \theta$ is equal to 90°, so, this expression reduces to $\sin^2(\Theta(t))$.

To summarize the steps above, the two polarizers and liquid crystal layer attenuate an incoming light with the transfer function shown below:

$$S(t) = 0.5sin^2(\Theta(t)) \tag{1}$$

In addition, this attenuated light is $\theta$-polarized.

As the signal $I \times S(t)$ travels towards the receiver, it is further attenuated by a factor $a$ due to its traveling distance.

Then, the receiver detects this signal plus the noise and interference coming from other sources, denoted by $b$. In the next sections, we show how our framework copes with noise and interference during the channel estimation process.

In the end, the received signal $r(t)$ is given by:

$$r(t) = I\ a\ S(t) + b \tag{2}$$

The final aim is to retrieve $S(t)$. In a SISO link, $S(t)$ is found by solving Equation 2. However, with MIMO, new terms will appear in the receiver's equation due to the interference from other channels[2].

[1]Malus' law states that the amount of light $I_o$ passing through a polarizer is dictated by $I_o = I_i Cos^2(\Delta\theta)$, where $I_i$ is the incoming light and $\Delta\theta$ is the angle difference between the polarizer and the polarized light.

[2]It is important to note that our model only includes intensity because VLC systems do not modulate the phase, as RF systems do.

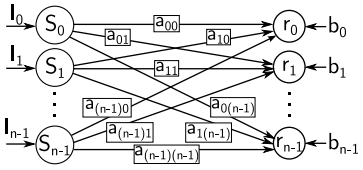


**Figure 3. A MIMO configuration.**

**Key novelty**. Polarization is widely used for modulation. In traditional systems, with optical fibers and lasers, only *one polarizer* is needed per channel because the transmitters are lasers (which are already polarized, coherent, and monochromatic) and the fibers are not exposed to interference from ambient light [10]. In passive VLC, most systems require *two polarizers* to cope with unpolarized light and to reduce interference from ambient light. The key insight of our mathematical model is to prove that using *three polarizers* enables MIMO even with interference and noise, which is a significant advantage because polarizers have almost a negligible cost. In the next section, we generalize our configuration to have multiple transmitters, and after that, we describe novel methods to reduce the inter-channel interference to obtain an operational MIMO system.

## 2.2 Multiple transmitters and receivers

As a corollary to Figure 2, we introduce the configuration in Figure 3 with $n$ transmitters and receivers. The transmitter $i$ modulates the intensity of its input light ($I_i$) with the transfer function $S_i(t)$. The attenuation of the light going from transmitter $i$ to receiver $j$ is $a_{ij}$. For brevity, we replace $I_i\ a_{ij}$ with $\hat{a}_{ij}$. Thus, in Figure 3, the signal at the $ith$ receiver is:

$$r_j = \sum_{i=0}^{n-1} \hat{a}_{ij} S_i + b_j \tag{3}$$

or in a matrix form for all receivers:

$$\begin{bmatrix} r_0 \\ r_1 \\ \dots \\ r_{n-1} \end{bmatrix} = \begin{bmatrix} \hat{a}_{00} & \dots & \hat{a}_{n-1,0} \\ \hat{a}_{01} & \dots & \hat{a}_{n-1,1} \\ \dots & & \\ \hat{a}_{0,n-1} & \dots & \hat{a}_{n-1,n-1} \end{bmatrix} \begin{bmatrix} S_0 \\ S_1 \\ \dots \\ S_{n-1} \end{bmatrix} + \begin{bmatrix} b_0 \\ b_1 \\ \dots \\ b_{n-1} \end{bmatrix} \tag{4}$$

This model captures a system of linear equations, where the matrix is called the channel matrix, and the aim is to solve for the vector $S$. *This system has a unique solution only if the channel matrix is non-singular, but creating a non-singular channel matrix is an open challenge in passive-VLC.* With *radio* backscattering (passive RF), the precise control of amplitude, frequency, and phase enables orthogonal (perfect non-overlapping) channels using various dimensions, such as frequency and coding [9, 14, 15]. LCs, on the other hand, only have a coarse non-linear output between two states, preventing them from employing these techniques.

There is only one passive-VLC study performing MIMO [21], which motivates our work and exposes the above *channel matrix* challenge. However, that study does not provide mathematical guarantees for a solution, nor does it try to tune the channel to obtain a non-singular matrix. As a result, it employs a MIMO system with high interference, resulting in rank-deficient channel matrices. Hence, *the key questions are whether it is possible to design a passive MIMO system with non-singular matrices, and if so, what is the best way to do it?* In the following subsections, we investigate these questions.

## 2.3 Passive-VLC and MIMO

To make the channel matrix non-singular, we need a careful analysis of its coefficients to reduce interference. To achieve that, we exploit two properties of light: polarization and color. Understanding the relation between these properties and the coefficients is key to designing a MIMO channel. Here, we explain this relation, and in Section 4, we investigate practical steps for their implementation.

*1) Polarization*: Following Section 2.1, the LCs in our model radiate $\theta$-polarized light. *A key insight of our work is to show that, in addition to the two polarizers mentioned before, adding a third polarizer to each receiver reduces sub-channel interference significantly.* In this part, we explain this concept by showing the effect of the third polarizer in three cases: *a)* a SISO channel, to demonstrate the basic principle; *b)* a MIMO channel with two sub-channels, and *c)* with several sub-channels, to demonstrate how the signals can be recovered despite interference. Overall, our approach provides a simple and effective solution to achieve MIMO with polarization.

***a) SISO channel.*** Consider the setup in Figure 4 with three polarizers, where the light coming out of the second polarizer (pol2) has an intensity of $\hat{a}S(t)$ and a polarization of $\theta$. If the third polarizer (pol3) is placed at angle $\beta$, the light faces a new attenuation factor equal to $cos^2(\theta - \beta)$. In total, the signal reaching the photodiode becomes:

$$r(t) = \hat{a}\ S(t) \cos^2(\theta - \beta) + b \tag{5}$$

where $\hat{a} = I\ a$, and $b$ includes the noise and interference measured by the receiver. It is important to note that if the transmitter and receiver are aligned, i.e. $\theta = \beta$, the signal strength is maximized. In that case, the SNR with 3 polarizers is higher than with 2. This occurs because the third polarizer reduces the intensity of the interference sources ($b$) by 0.5x. The expert reader could argue that there is no advantage in adding a third polarizer. Instead, the second polarizer could be removed from the LC and placed on the receiver's PD, as done in some prior works [8, 21]. However, we will see that the benefit appears when multiple transmitters are used.

***b) MIMO link with two orthogonal sub-channels.*** Suppose there are two channels indexed 0 and 1, both having the configuration shown in Figure 4, but with different polarization angles. Channel 0 has polarizations $pol2 = pol3 = \gamma$, and channel 1 has $pol2 = pol3 = \gamma^{\perp}$ (perpendicular to $\gamma$). The light reaching each receiver is the sum of the light from both transmitters. So, the received signal in channel 0 is:

$$\begin{aligned} r_0^{3pol}(t) &= \hat{a}_{00}\ S_0(t) \cos^2(\gamma - \gamma) + \\ &\quad \hat{a}_{10}\ S_1(t) \cos^2(\gamma^{\perp} - \gamma)\ + b_0 \\ &= \hat{a}_{00}\ S_0(t) + b \end{aligned} \tag{6}$$

The key advantage of our 3-polarizer method is that we create orthogonality: $r_0$ only captures transmitter 0, and vice-versa. This occurs because the first cosine term maintains the intended signal, as in the SISO case, but the second cosine term eliminates the interference of $S_1$. *Using a third polarizer creates two orthogonal channels*, with the SNR of each MIMO sub-channel being *at least*

Seyed Keyarash Ghiasi
Delft University of Technology and Marco Zuniga
Delft University of Technology

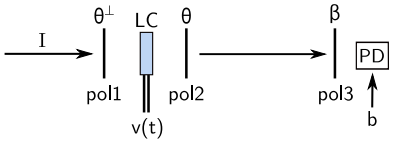


**Figure 4. A SISO link with three polarizers**

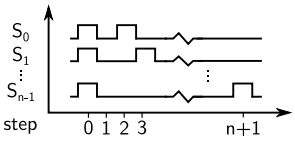


**Figure 5. The preamble of our MIMO system.**

equal to the SISO channel[3] (Equation 2). If each sub-channel used only two polarizers, pol1 and pol2, the signal received by channel 0 would still contain the interference from channel 1.

$$r_i^{2pol}(t) = \hat{a}_{00}\, S_0(t) + \hat{a}_{10}\, S_1(t) + b$$

Intuitively, our approach creates two independent channels by forcing single polarization directions that are orthogonal. Next, we generalize this concept for more channels and expose its limitations.

***c) MIMO with several sub-channels.*** Having more than two sub-channels means that the polarization angles can no longer be mutually orthogonal. That is, there will be interference. However, using *pol3* allows for reducing the interference, which leads to non-singular matrices if the system is carefully designed. The key intuition in the most general case is as follows: without *pol3*, the received signals are the ones shown by Equation 3, adding pol3 multiplies the receiver signal by $cos^2(\theta_k - \beta_i)$. Considering the signals from all transmitters to receiver $i$, the effect of *pol3* leads to

$$r_i = \sum_{k=0}^{n-1} \hat{a}_{ki} S_k(t) cos^2(\theta_k - \beta_i) + b_i \tag{7}$$

These new cosine terms will appear in the channel matrix of Equation 4, resulting in a new degree of freedom that affects the channel matrix and its non-singularity. Two important questions are how to determine the maximum number of separable channels, and how the selection of $\theta$s and $\beta$s affects the link. We tackle these questions in the next section.

*2) Color*: Ambient light contains multiple colors. A recent study uses dichroic filters to divide sunlight into two channels [6]. Those filters have little co-channel interference but are expensive (about 30 USD). We use the simplest color filters, less than 1 USD per A4 sheet [1], which have more co-channel interference. These filters require a mathematical framework to build an invertible channel matrix with LCs.

In the next sections, we provide a thorough analysis of color filters. Similar to polarization multiplexing, we do not assume a full separation between color bands, i.e. the color channels can overlap. In addition, we will show that the *polarization* and *color* approaches can be combined in a hierarchical manner, allowing for even more multiplexed channels without substantially increasing the interference.

## 2.4 Signal Quality

Up to here, we have looked into methods that can make the channel matrix invertible to guarantee a solution for Equation 4. However, this does not guarantee a *good enough* separation between sub-channels. To have a metric showing the signal separation among transmitters, we use the *condition number* of the MIMO channel. *Note that in RF communications, the condition number is used to benchmark MIMO systems because the focus is on channel separation. Other metrics such as SNR or BER are used afterwards to measure the link quality once the channel separation has been analyzed. In our evaluation section, we follow the same process. First, we analyze the condition number and then the BER.*

The condition number is defined by the equation below:

$$\text{cond} = |\frac{\lambda_{max}}{\lambda_{min}}| \tag{8}$$

where $\lambda_{max}$ and $\lambda_{min}$ are the maximum and minimum eigenvalues of the channel matrix. A condition number ranges from 1 to infinity, with lower numbers showing less interference between the channels. In the following section, we discuss how polarization and color affect the channel's condition number, as well as ways to select the *best* combination of parameters to obtain a low condition number.

# 3 Passive MIMO channel

After formalizing a model for a passive MIMO link, we now tackle the implementation challenges by answering two questions: first, how can the passive MIMO channel be practically estimated? second, what are the conditions, performance, and limitations of using polarization and color to make multiplexed channels?

## 3.1 Channel estimation

In the MIMO system of Figure 3, the photodiodes measure superimposed and attenuated signals coming out of each transmitter ($S_i$). These signals can be recovered only if the receiver $r_i$ knows the channel matrix as well as the noise values $b_i$. In this section, we present a way to obtain those parameters. To achieve that, a custom-designed preamble is sent by the transmitters to perform the channel estimation process. Below, it is explained how to form such a preamble.

*3.1.1 A preamble for channel estimation.* The channel matrix has $n^2$ variables $\hat{a}_{ij}$ and $n$ variables $b_i$. To solve it, we send a known preamble of length $n + 2$. A sample preamble is shown in Figure 5, where $S_i = 1$ means that the $i^{th}$ transmitter is set to its transparent state, and vice versa. Following the figure's timeline, the steps taken to form the preamble are:

step 0: all $S_i$ are set to 1. This is used only to mark the start of a preamble. It has no significance in the channel estimation.

step 1: all $S_i$ are set to 0 in Equation 4. This results in the channel matrix to be multiplied by a zero vector, therefore $b_i$ will be equal to the measured $r_i$ for every $i$.

steps 2 to n+1: in each of these steps, only one of the transmitters is set to 1, and all other $S_i$ are set to 0. In addition, no transmitter is set to 1 more than once. Each step results in $n$ equations, and since there are n steps (2 to n+1), there are $n^2$ equations to solve the channel matrix.

After solving Equation 4, we have to make sure that the channel matrix is non-singular. We also need a low-condition number to maintain enough distance between channels. Next, we describe how

[3]We state 'at least' because the noise and other ambient interference is lowered by 0.5 by the third polarizer.

an arrangement of polarization and color filters defines the channel matrix, and we investigate the conditions to have a recoverable MIMO channel.

## 3.2 Polarization multiplexing

Our approach using three polarizers enables more parallel channels, but there is an upper limit to the number of channels that can be multiplexed. We first find this upper limit, and then, we run a simulation based on our model to find the configuration with the lowest condition numbers.

Considering transmitter $i$ and receiver $j$ in a multi-channel platform, let us denote $p_{ij} = \cos^2(\theta_i - \beta_j)$ as the attenuation caused by the third polarizer at the receiver (pol3 in Figure 4). As a result, the channel matrix has to be updated to:

$$H = \begin{bmatrix} \hat{a}_{00}p_{00} & \cdots & \hat{a}_{(n-1)0}p_{(n-1)0} \\ \hat{a}_{01}p_{01} & \cdots & \hat{a}_{(n-1)1}p_{(n-1)1} \\ \cdots & & \\ \hat{a}_{0(n-1)}p_{0(n-1)} & \cdots & \hat{a}_{(n-1)(n-1)}p_{(n-1)(n-1)} \end{bmatrix} \quad (9)$$

In addition, since all sub-channels come from adjacent transmitters (i.e. a single transmitter with multiple LCs), we can assume that all $a_{ij}$s (the attenuations due to distance) have the same (approximate) value $a$. In this case, the elements of column $i$ will be equal to $I_i \times a \times p_{ij}$. Thus, the prior matrix can be written as:

$$H = a^{n^2} \begin{bmatrix} I_0 p_{00} & \cdots & I_{n-1}p_{(n-1)0} \\ \cdots & & \\ I_0 p_{0(n-1)} & \cdots & I_{n-1}p_{(n-1)(n-1)} \end{bmatrix} \quad (10)$$

To see if this matrix is invertible, we have to find its determinant. One can prove that for $n \geq 4$ the determinant is zero[4] regardless of the values of $\theta$ and $\beta$. This means that with this approach, a maximum of 3 channels can be polarization-multiplexed without making the channel matrix singular. In addition, for $n \leq 3$, the matrix is invertible even if $\theta_i$ (at the transmitter) and the corresponding $\beta_i$ (at the receiver) are different. In Section 2.3, $\theta_i$ and $\beta_i$ were set to the same angle for the 2-channel example to clarify the idea. In practice, this is not necessary, which has a *strong advantage in a real implementation* because *it means that the polarizers at the transmitter and receiver do not need to be perfectly aligned.* The only condition to guarantee that the matrix is invertible is that no two $\theta_i$s or two $\beta_j$s are the same.

*3.2.1 Maximizing channel separation.* Non-singularity is a necessary but not sufficient condition to have a working MIMO channel. The channel matrix must also have a sufficiently low condition number to reduce inter-channel interference. To identify the angles that minimize the *condition number*, we resort to numerical analysis. The analysis has two steps, first, we identify the lowest condition number for two channels and then, we minimize the condition number once the third transmitter is added.

For two transmitters, setting one set of angles to 0° ($\theta_0 = \beta_0 = 0°$) and the other set to 90° ($\theta_1 = \beta_1 = 90°$) leads to the following diagonal channel matrix, i.e. a (perfect) orthogonal channel:

$$H = a^2 \begin{bmatrix} I_0 & 0 \\ 0 & I_1 \end{bmatrix} \quad (11)$$

In this case, the condition number is $\frac{max(I_0,I_1)}{min(I_0,I_1)}$, which has the lowest possible value of 1 if $I_0 = I_1$. This analysis proves the derivation given in Section 2.3 for the (perfect) orthogonality of the dual channel with three polarizers.

[4]We used Wolfram Alpha for the proof.

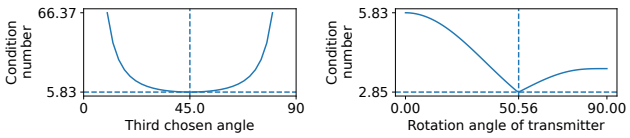


**(a) With three LCs: two fixed at 0° and 90°, and the third angle sweeps from 0° to 90°.**

**(b) With three channels (0°, 45°, 90°) and the roll angle sweeps from 0° to 90°.**

**Figure 6. Analysis of condition numbers**

For 3 transmitters and receivers, we keep the 0° and 90° angles, and add a third angle $\theta_2 = \beta_2 = x$. The variable $x$ is swept from 0° to 90°, and the resulting condition number of the 3×3 channel matrix is shown in Figure 6a. In this Figure, the minimum condition number (5.83) happens when x = 45°. Hence, for a 3-channel MIMO, the angles need to be 0, 45 and 90 degrees. To put the condition number in perspective, we found that in our system, values below 10 lead to a tolerable amount of interference. Such reduction of interference has a major impact on modulation: *compared to the SoA studies, which have proposed increasingly complex modulation methods* to increase the data rate, *our quasi-orthogonal channels allow the use of the simplest modulation method (OOK)* in a reliable manner, and the only trade-off is adding inexpensive (few cents) polarizing sheets and more photodiodes.

*3.2.2 Roll rotations and condition number.* In the method above, we assume that the transmitters and receivers are aligned, that is, there is no rotation in the roll axis. However, in real scenarios, the receiver may not always be aligned with the transmitter, hence, we have to investigate the sensitivity of the link to rotations. To analyze these rotations, we add an offset $\beta_r$ to the polarizers in the receiver. In that way, the polarizing angles of the transmitter are $\theta_0 = 0°$, $\theta_1 = 45°$, and $\theta_2 = 90°$, and the angles of the receiver are $\beta_0 = \beta_r$, $\beta_0 = 45° + \beta_r$, and $\beta_0 = 90° + \beta_r$. Next, we sweep $\beta_r$ from 0° to 90°, and the condition numbers are calculated at each step. The result of this analysis is shown in Figure 6b, which shows that roll rotations have no detrimental effects, as the condition number stays below 5.83. In fact, a roll of about 50° provides the best performance. In our evaluation, we observed that with condition numbers below 5, we can obtain links with zero or close to zero bit-error rate (BER), thus, a misalignment in the roll axis does not impact our system.

## 3.3 Color multiplexing

As stated before, the bandwidth of visible light is wide. To use the bandwidth more efficiently, we can multiplex channels using color filters. In that case, the same principle applies as with polarization: the color channels do not need to be orthogonal, and can have an overlap as long as the channel matrix has a sufficiently small condition number. To analyze the color domain, we follow the same procedure as with polarization, and find the best color filters for MIMO.

*3.3.1 Channel derivation.* To describe our approach with colors, let us consider the Tx-Rx pair shown in Figure 7a. The transmitter consists of an LC cell, shown by the grey box, and a color filter afterwards. The LC attenuates the input light by a factor of S(t) (Equation 1) and the color filter exerts an attenuation $c_i$, which is dependent on the filter's spectrum. Next, the signal travels to the receiver, where it encounters another color filter (green) with

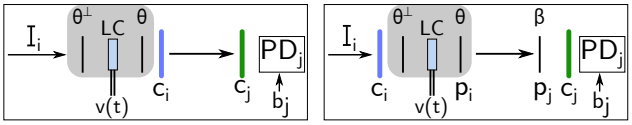


**(a) A Tx-Rx pair using only color**

**(b) A Tx-Rx pair using both polarization and color.**

**Figure 7. Tx-Rx models using color and polarization.**

**Table 1: Condition numbers for "n" color filters (r:red, b:blue, c:cyan, g:green, v:violet, l/dp:light/dark pinks)**

| 2-color | 3-color | 4-color |
|---|---|---|
| (r,b):1.13 | (r,g,b):4.79 | (b,g,lp,dp):14.91 |
| (r,c):1.85 | (b,g,dp):5.88 | (r,g,v,lp):16.93 |
| (r,g):1.88 | (r,g,v):7.10 | (r,g,b,lp):19.08 |

attenuation factor $c_j$. If the spectrum of the filters at the transmitter and receiver match, then $c_j = 1$. Combining the effects of the color filters, the signal is attenuated by the factor $c_{ij}$. This means that each pair of color filters makes for a unique attenuation factor, and this characteristic makes it possible to build a MIMO channel. Contrary to the polarization case, where the transfer function $S(t)$ is attenuated by the cosine functions; for the color case, $S(t)$ is attenuated by the factor $c_{ij}$, which leads to the following channel matrix:

$$H = \begin{bmatrix} \hat{a}_{00}c_{00} & \dots & \hat{a}_{(n-1)0}c_{(n-1)0} \\ \dots & \dots & \dots \\ \hat{a}_{0(n-1)}c_{0(n-1)} & \dots & \hat{a}_{(n-1)(n-1)}c_{(n-1)(n-1)} \end{bmatrix} \quad (12)$$

In the next part, we analyze these coefficients for different color filters to identify the best combination.

*3.3.2 Color selection.* The color selection could be done with a numerical analysis, similar to the polarization case, but this requires knowing the spectral response of the color filters. The filters that we use, however, are inexpensive, a few cents per receiver, and they do not have a datasheet. Hence, we pursue the following empirical approach.

*1) Benchmark all color filters*: We use a set of 10 filters: red, green, blue, cyan, light pink, dark pink, orange, lime, yellow, violet. First, we build a testbed with 10 LCs and 10 photodiodes, each channel masked with a different color filter. Then, we follow the preamble mechanism presented in Section 3.1.1, where each transmitter is activated only once, while the others remain off. This approach permits obtaining the elements $c_{ij}$ for all pair-wise color combinations, and hence, building a complete channel matrix.

*2) Iterate the design space:* Based on the channel matrix, we can build sub-matrices to obtain any $m$-combination of colors, with $m$ ranging from 2 to 10. For each combination, we use the columns and rows corresponding to the selected colors.

*3) Find the optimum solution*: We calculate the condition numbers for all the combinations to identify the maximum number of channels we can obtain and the best filters to use.

Following the above steps, we identify that using 4 color channels already provides condition numbers close to 15 or higher, which means that the maximum number of channels that we can reliably use with *inexpensive filters* is three. Table 1 shows that the best color combination for two channels is red and blue; this mixture provides an almost orthogonal channel with a condition number of 1.13. For a 3-color channel, the best combination is red, green, and blue, providing a condition number of 4.8, which is close to the condition number using three polarization-multiplexed channels.

**Scalability.** Overall, our analysis shows that we can have three *reliable* channels in each domain, polarization and color. In traditional optical fiber systems, the number of channels using polarization can be increased to four channels (or more) using some form of channel coding [10]. The number of color channels can be increased with filters that have a sharper response. Those approaches could be used with our method, but our goal is to provide the first principled model for MIMO with passive VLC. In the next section, we show how these two domains can be combined to obtain nine channels.

## 4 Designing a practical channel

In this section, we propose practical modulation methods using the insights of the previous sections. We will show that, depending on the configuration of the transmitter, two modulation methods can be applied: *flat* or *hierarchical*.

### 4.1 A multi-layered channel

Polarization and color are independent characteristics of light, which means they can be used simultaneously to increase channel capacity. A platform with $m$ colors and $n$ polarizations can multiplex $m \times n$ channels. One Tx-Rx pair of such channel is shown in Figure 7b, where the (color, polarization) pair for the transmitter is denoted as ($c_i$,$p_i$), and for the receiver as ($c_j$,$p_j$). Following the analysis of Section 3, we consider 3 polarizations (0°, 45°, 90°), and 3 colors (red, green, and blue) to build a maximum of 9 channels.

To make a MIMO channel with the mentioned properties, we propose two approaches: *flat*, and *hierarchical*. The latter results in better channel separation, but it can only be used if both color and polarization are used. To avoid over-complicating our example, we will discuss the case of 2 polarizations ($p_0$ and $p_1$) and 2 colors ($c_0$ and $c_1$), although we can extend it to a higher number of colors and polarizations.

### 4.2 Communication system

In our example with four transmitters and receivers, each Tx-Rx pair has a unique $p_{ij}c_{ij}$ combination, as shown in Figure 8a. To estimate the channel matrix, proper preambles have to be designed. Next, we explain the difference between the *flat* and *hierarchical* preambles.

*4.2.1 "Flat" modulation.* In this approach, the preamble is constructed in the same way as the case with only polarization or color multiplexing, which was explained in Section 3.1. Here, we quickly recap the steps. As shown in Figure 8b, first, all the transmitters send a '1' (to mark the start), then, all transmit a '0' (to obtain the noise $b_i$), and finally, each transmitter sends a '1' in a round-robin fashion to solve the $n \times n$ channel matrix (in this case $n = 4$).

*4.2.2 "Hierarchical" modulation.* When colors and polarizations are used jointly, the channel can be demultiplexed in two steps. First, the channel is considered to be only color-multiplexed, and then, only polarization-multiplexed. This approach has several advantages compared to the *flat* mode, as we discuss later. But before that, we modify the mathematics of Section 2 to model the hierarchical approach.

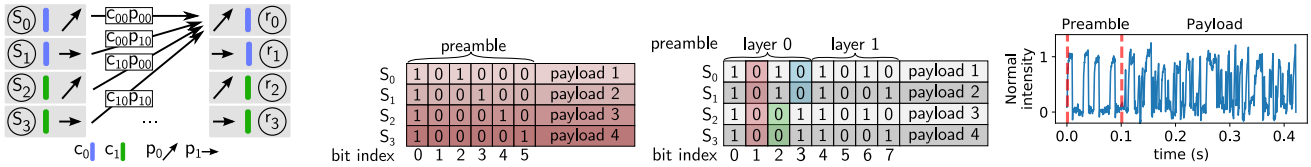


(a) Setup combining colors and polarizers.

(b) The *flat* preamble for 2 polarizations and 2 colors.

(c) The *hierarchical* preamble for 2 colors and 2 polarizations.

(d) A demultiplexed channel from 9 Tx-Rx pairs.

**Figure 8. Combination of polarization and color: setup and preambles**

Considering the example of two polarizations and two colors in Figure 8a, the equations for the receivers are:

$$\begin{aligned} r_0 &= c_{00}(S_0p_{00} + S_1p_{10}) + c_{10}(S_2p_{00} + S_3p_{10}) + b_0 \\ r_1 &= c_{00}(S_0p_{01} + S_1p_{11}) + c_{10}(S_2p_{01} + S_3p_{11}) + b_1 \end{aligned} \tag{13}$$

and

$$\begin{aligned} r_2 &= c_{01}(S_0p_{00} + S_1p_{10}) + c_{11}(S_2p_{00} + S_3p_{10}) + b_2 \\ r_3 &= c_{01}(S_0p_{01} + S_1p_{11}) + c_{11}(S_2p_{01} + S_3p_{11}) + b_3 \end{aligned} \tag{14}$$

If we rename the expressions inside the parentheses to

$$\begin{aligned} S'_0 &= S_0p_{00} + S_1p_{10} \qquad & S'_1 &= S_2p_{00} + S_3p_{10} \\ S'_2 &= S_0p_{01} + S_1p_{11} \qquad & S'_3 &= S_2p_{01} + S_3p_{11} \end{aligned} \tag{15}$$

We observe that the *polarization matrix* $\begin{bmatrix} p_{00} & p_{10} \\ p_{01} & p_{11} \end{bmatrix}$ is exposed, but solving it requires knowing the values of $S'_i$. To obtain those values, we can re-arrange the receivers in Equations 13 and 14 to:

$$\begin{aligned} r_0 &= c_{00}S'_0 + c_{10}S'_1 + b_0 \qquad & r_1 &= c_{00}S'_2 + c_{10}S'_3 + b_1 \\ r_2 &= c_{01}S'_0 + c_{11}S'_1 + b_2 \qquad & r_3 &= c_{01}S'_2 + c_{11}S'_3 + b_3 \end{aligned} \tag{16}$$

This formulation only exposes the *color matrix* $\begin{bmatrix} c_{00} & c_{10} \\ c_{01} & c_{11} \end{bmatrix}$. If the transmitter activates only $S'_0$ and $S'_2$ in one cycle (blue filter), and only $S'_1$ and $S'_3$ in the next cycle (green filter), the system can obtain all of the color coefficients $c_{ij}$, and in turn all $S'_i$. Then, with the values of $S'_i$, the system could first activate only one polarization direction ($S_0$ and $S_2$), and then other direction ($S_1$ and $S_3$) to obtain all the coefficients $p_{ij}$. This approach would result in solving two *flat* 2×2 matrices instead of solving a 4×4 matrix. Next we explain how we design a preamble to activate the $S'_i$ variables as desired.

*4.2.3 Forming a hierarchical preamble.* Considering the example with two polarizations and colors, the corresponding hierarchical preamble is shown in Figure 8c. Below, we describe how it is generated.

*step 1 & 2)* Similar to the flat case, first, all transmitters send '1' to mark the beginning. Then, all transmitters send '0' to obtain the noise $b_i$.

*step 3)* To obtain the coefficients of the first hierarchical layer (color in our example), we need to generate the signals $S'_i$ in Equation 16 that turn on one color channel at a time. To achieve that, we first set $S_2$ and $S_3$ to 0 to turn off the green channel (highlighted in Figure 8c), and then we set $S_0$ and $S_1$ to 0 to turn off the blue channel. This operation leads to a *flat* 2×2 matrix where the $c_{ij}$ coefficients are derived.

*step 4)* To mark the beginning of the second layer, we repeat steps 1 and 2 (all Tx are first on and then off).

*step 5)* To obtain the polarization coefficients, we need to generate the $S'_i$s that turn on one polarization direction at a time in Equation 15. To achieve that, we first turn off $S_1$ and $S_3$, and then we turn off $S_0$ and $S_2$. This operation leads to a *flat* 2x2 matrix where the $p_{ij}$ coefficients can be derived.

*4.2.4 Comparing the hierarchical and flat approaches.* The advantages of the hierarchical configuration are discussed in three domains: preamble length, computational complexity, and SNR. Our comparison below assumes $m$ polarizations and $n$ colors, resulting in $m \times n$ parallel channels.

***1) Preamble lengths:*** In a flat approach, the preamble has a length equal to the number of parallel channels plus two signaling bits, which leads to $m \times n + 2$ bits. In the hierarchical approach, the preamble has a length of $m + n + 4$ bits, thanks to the grouping of channels and their parallel calculations. Hence, the hierarchical approach is more efficient in terms of its preamble length.

***2) Computational intensity:*** In both methods, the computation-intensive operations are matrix inversion and multiplication. In the flat approach, we need the inverse of an $m \times n$ matrix, which takes $(mn)^3$ operations. In addition, a matrix-vector multiplication is needed for each data sample, which is proportional to $(nm)^2$ operations. On the other hand, in a hierarchical setup, there are two steps. In the first step, there is an $m \times m$ matrix, and in the next step an $n \times n$ matrix (or vice versa, depending on the design). This results in a total of $m^3 + n^3$ operations for matrix inversion. In addition, for matrix multiplications the system needs $m \times n^2 + n \times m^2 = mn(m+n)$ operations. If $m = n$, we see that the hierarchical approach (with complexity $4m^3$) is significantly more efficient that the flat approach (with complexity $m^6 + m^4$).

These complexities might still seem *too* high for low-end platforms, such as microcontrollers. However, our theoretical model does not require repetition of channel matrix inversion as long as the light spectrum remains constant. Under these conditions, the same inverted matrix can be used, even if light intensities change. The latter case only results in changing the offset value of the demodulated data.

***3) Signal quality:*** With the hierarchical approach, fewer number of parallel channels have to be considered at each demultiplexing step. In Section 6, we will empirically show that the hierarchical approach yields a lower condition number, resulting in a higher SNR.

## 4.3 Modulation & Demodulation

Up to here, we only considered the demultiplexing of sub-channels. In addition to being multiplexed, the signals have to be modulated before transmission, as explained below.

*4.3.1 Modulation.* Each packet has only two fields, preamble and payload, and they are modulated in different ways:

**Preamble.** In the preamble, the most important requirement is to obtain accurate coefficients for polarization and color. Due to this reason, when an LC cell changes its state, we let it run until it

reaches its plateau. An example is shown in Figure 8d, which shows one of the sub-channels in a MIMO system with 9 sub-channels. For this LC, we wait 10 ms for each preamble bit, so that both the slow behaviour of LCs and the triggering jitter between different LCs are overcome. For this link with 9 sub-channels, the total preamble time is 100 ms (there are 10 bits in the preamble: 3 colors, 3 polarizations, plus 4 bits of '1' and '0'). Once created, this preamble does not need to be renewed at each transmission as long as the channel stays the same. This means that the transmitter is not burdened with any additional processing.

*It is important to note that the preamble does not need to be transmitted again for different light intensities.* Our demultiplexing method uses relative values of the preamble, so, when the light intensity changes, it is similar to multiplying the channel matrix by a fixed factor, which causes the demultiplexed data to be scaled and shifted by a constant value. If a link is designed without sending the full preamble before every packet, it still has to send the preamble's first bit (all LCs on) for two reasons: a) to mark the start of a payload, and b) to provide a reference to normalize the payload signal after demultiplexing. This normalization allows the use of demodulation thresholds obtained with preambles at different light intensities.

**Payload.** Once the preamble is sent, the requirement of the system changes to increasing the data rate. The transmitter does not need to wait for a full contrast (plateau); so long as a signal is above a given threshold, the symbol can be deemed a '1'. Since our framework reduces co-channel interference significantly, we can rely on this basic thresholding strategy, and use it with the simple modulation method of OOK. For the LC in Figure 8d, which has a fall time of 0.7 ms and a rise time of 2.5 ms, a bit period of 1 ms (1 kbps) was enough to provide signals with sufficient peak height.

**Clock transmission.** As seen above, the duration of bits in the preamble (10 ms) are longer than the bits in the payload (1 ms). This means that if the payload is not long enough, the data rate drops due to the significant time allocated to the preamble. Hence, the payload's length must be long to amortize the preamble's effect. Thus, in our evaluation, we send from 300 to 1000 bits in one payload, which poses another risk: since OOK does not have embedded synchronization, as the payload gets longer, the demodulation becomes susceptible to clock recovery failures. Using an encoding mechanism such as Manchester is not favourable either, as it reduces the data rate by a factor of 0.5. To overcome this, we used channel 0 to transmit the data clock. This channel has repetitive data, thus reaches a steady state very fast. In that manner, the clock peaks are at the same height, and can be found with a simple peak-finding algorithm. *Using a channel for clock transmission is a simple technique but it was not used in any prior passive-VLC study. In our case, this design makes sense because we have nine channels and it is not a significant overhead to use one of them as a clock.*

## 4.4 Demodulation

The demodulation follows simple steps.

*step 1:* We apply a 3rd-degree low-pass Butterworth filter with a bandwidth higher than the clock frequency of the payload. This filter removes most of the high frequency noise.

*step 2:* The preamble is located by detecting the first strong peak in the signal, and then, the entire preamble (between the red bars in Figure 8d) is used to obtain the channel matrix.

*step 3:* The clock signal is extracted from the 'payload' of the first channel, and used to determine the location of data bits in all other channels.

*step 4:* Decoding the payload requires a threshold. Anything above the threshold is considered a '1', and otherwise a '0'. The threshold depends on the LC cell's bandwidth and modulation period. For the LC in Figure 8d, a full switching cycle takes more than 3 ms, but to increase the data rate we use a period of 1 ms. For that period, we found empirically that a threshold of 0.2 (normalized with respect to the maximum signal strength in the preamble) is reliable to decode data.

Overall, the important takeaway is that a solid theoretical foundation enables the design of simple (de)modulation processes, compared to the SoA, which relies on heuristics to develop complex modulation schemes.

# 5 Platforms

We tested our theoretical framework by developing a backscattering communication link. The link's configuration is shown in Figure 9a. Our setup assumes the standard backscattering scenarios in the SoA, where *objects* with lights –such as ceiling luminaires, desk lamps or car lights– gather data from nearby *surfaces*. In our prototype, the light radiated by the object is not modulated, however, upon reaching a surface with LCs and retroreflectors, this light is modulated and backscattered to the object, which has photodiodes to decode the passive link.

## 5.1 Transmitter (Surfaces)

Our MIMO transmitter considers two types of liquid crystals: a) Twisted Nematic (TN) cells, and b) Pi cells. TN cells are cheaper, easier to drive, and more power efficient, however, they have limited bandwidth. We used TN cells with a bandwidth of about 125 Hz (2 ms charging time and 8 ms discharging time), and Pi cells with a bandwidth of about 400 Hz (0.7 ms charging time and 2.5 ms discharging time). To drive these cells, we use off-the-shelf STM32 microcontrollers combined with amplifying circuits.

For both TN and Pi cells, we build a panel of $3 \times 3$ LCs, with 3 different polarizations and 3 different colors. All cells are mounted on retroreflectors, as done in the SoA [13, 19, 20], to send the modulated light back. Using retroreflectors does not degrade the link, as these devices preserve both, the polarization and color of light. The transmitters with TN and Pi cells are shown in Figure 9b.

## 5.2 Receiver (Object)

Our receiver consists of 9 photodiodes (PDs) mounted on a 3D stand. The light source is a 13 W flashlight, which is similar to the 12 W lamp used in Retro-VLC [13]. The color filters and polarizers of the transmitting LCs are also placed in front of each PD. In our evaluations, we use the same number of PDs as the number of transmitting channels. The receiver as well as the flashlight on which it is mounted are shown in Figure 9c.

## 5.3 Cost and energy consumption

The cost and power consumption of the platforms are shown in Table 2. The color filters and extra polarizers add a negligible cost, less than 1 USD. Contrary to the TN cells, the Pi cells add the most cost as a trade-off for their higher speed: a combination of their transmitters and receiver array costs around 250 USD.

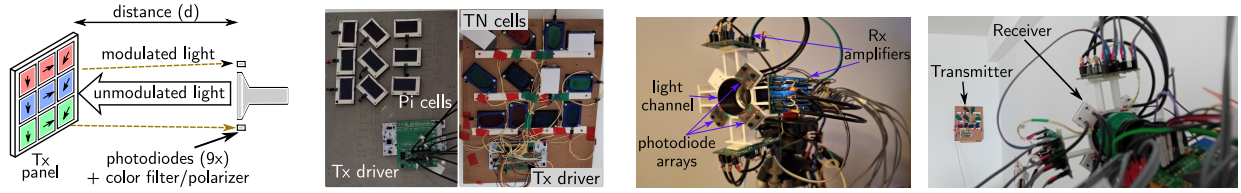


(a) Link's configuration (b) Transmitters (c) Receiver (d) Communication link

**Figure 9. Platforms: configuration, transmitters, and receivers.**

**Table 2: Costs and power consumption**

| | Component | Pi cell Tx | TN cell Tx |
|---|---|---|---|
| Transmitter | LC cell | 9 × 15 USD | 9 × 4 USD |
| | Nucleo board | 17 USD | 17 USD |
| | Power consumption | 450 mW | 0.37 mW |
| Receiver | Photodiodes | 9 × 0.5 USD | |
| | Receiver boards | 9 × 7 USD | |
| | Power consumption | 150 mW | |

We tried selecting LCs with responses similar to the ones reported in the SoA. The response of the TN cell is close to the ones used in [19], and the Pi cell's response is close to the ones used in [7, 20]. We, however, did not optimize the hardware to obtain a sub-milliWatt power consumption. Between the two types of cells, we found that the Pi cells are faster but they consume more energy because they require higher frequency pulses (2 kHz) oscillating at amplitudes of ±10V for the opaque state, and ±5V for the transparent state. On the other hand, the TN cells only require 0V and 4V to oscillate at frequencies below 400 Hz. *Building platforms with the fast but low-power cells reported in [20], as well as their optimized driving circuits, would be the best combination of our work and the SoA.*

# 6 Evaluation

In this section, we assess the system's performance in several aspects such as BER, distance, and condition number.

## 6.1 Flat versus hierarchical modulation

In Section 4, we stated that there are three advantages when it comes to hierarchical modulation: a lighter preamble, lower computational complexity, and better performance. We already showed the first two advantages analytically and left the third to an empirical evaluation. To do this comparison, we run experiments with our basic setup described below:

***Experimental setup:*** To implement the multiplexed link, we place our setup in a low-light office environment of about 100 Lux. We maximize the receiver's gain such that it stays below saturation considering the ambient light and transmitted signal. The link is shown in Figure 9d. In this Figure, the transmitter is 3 meters away from the receiver, however, we change the distance for other experiments.

To compare the two modulation approaches, we do experiments in which 4, 6, and 9 channels are multiplexed at a distance of 2 m. For the *flat* approach, we report the condition number of the channel matrix, and for the *hierarchical* approach, first, we calculate the condition numbers for color and polarization separately, and report the bigger of the two, as this determines the overall quality of the channel separation. The results are shown in Figure 10a. As is evident, the *hierarchical* approach outperforms the *flat* one, specifically for 9 channels, in which the *flat* approach is almost non-recoverable. Also, in all experiments, the *hierarchical* condition number stays below 5, guaranteeing a *good* demultiplexing of the channels.

## 6.2 Bit error rate

The condition numbers capture channel separation, but the link quality needs to be assessed by its BER. Using the *experimental setup* described before, we evaluate the two transmitter types: Pi cells and TN cells. For each type of cell, we run experiments with constant and varying light. Below, we describe each scenario separately.

*6.2.1 Pi cells.* To evaluate these cells, we conduct experiments at 1, 1.5 and 2 meters, operating all of the 9 parallel channels. For the three distances above, the light intensity at the LC transmitter is 3.5, 1.3, and 0.9 kLux, respectively. Following Section 4.3, we set the preamble's bit duration to 10 ms, and for the payload's period, we use three settings of 1, 1.5, and 2 ms per channel. Also, as stated in Section 4, we assign one channel to clock transmission, thus, the effective data rates –considering the longer preamble and that one LC is used as clock– are 6.8, 4.7, and 3.7 kbps. In our tests, we send packets of 500 or 1000 randomly generated bits, and calculate the BER. These results are shown in Figure 10b. At 1.5 meter, the BER for 3.7 and 4.7 kbps is almost 0, and for 6.8 kbps stays below 1%. However, as the distance increases, the BER of the low and mid rates increases to about 3 to 4%, and the link with the highest rate is not recoverable.

At 1 meter, the results might seem counter-intuitive: we expect to see lower BERs after decreasing the distance. However, at this distance, some of the transmitters go out of the field-of-view of the receivers. Thus, the high BER is due to the demultiplexing, and not the demodulation. This issue could be solved by using a more compact transmitter putting all of the LCs in the FoV of the photodiodes. This is discussed in 8.

*6.2.2 TN cells.* These cells are inherently slower than Pi cells: their maximum bandwidth for a full contrast is 125 Hz. Here, we experiment at three distances: 1, 2, and 3 meters, using a preamble clock of 15 ms and three payload clocks: 5, 6, and 10 ms. Similar to the Pi cells, we dedicate one channel as clock, hence, the effective data rates are 1.5, 1.2, and 0.7 kbps. In these tests, the payloads consist of 300 random bits. The BER results are shown in Figure 10c. At 2 meters, the BER stays at 0.0% for 0.76 and 1.2 kbps, and at 3 meters, it is still 0 for the slower setting and stays under 1% for the mid data rate. For the faster setting, the BER is close to 1% at 2 m. Similar to the Pi cells, at 1 meter, there is an increase in the BER. However, this increase is more substantial compared to Pi cells. This is because the TN cells are bigger and more distant to each other. Thus, the transmitters go out of the FoV of the receivers faster, resulting in poorer demultiplexing at the same distance. As stated before, this is

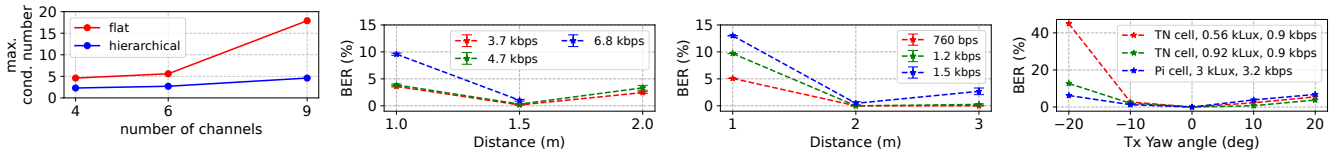


(a) Flat vs. hierarchical. (b) BER using Pi cells. (c) BER using TN cells. (d) BER vs. yaw angles.

**Figure 10. Evaluation results.**

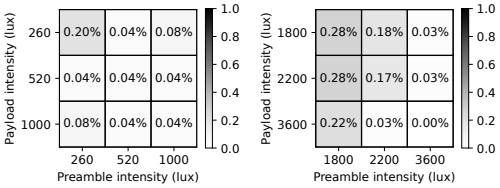


(a) TN cell, 0.9 kbps (b) PI cell, 3.2 kbps

**Figure 11. BER when the preamble and the payload are captured under different light intensities.**

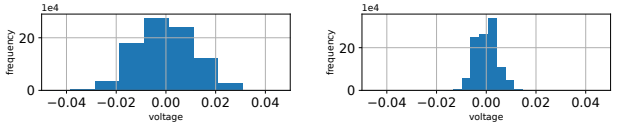


(a) without the third polarizer (b) with the third polarizer.

**Figure 12. Noise effect of the third polarizer.**

not a fundamental limitation, custom LCs can be much smaller. For example, in projectors, arrays of LCs are built with millimeter-size. Smaller LCs would solve the limitations of our transmitters.

It is important to note that the slow TN cells reach a lower BER despite being modulated at 1.6× their bandwidth and for longer distances. We attribute this to the following reasons:

*reason 1:* The TN cells have a larger surface area to reflect back more light. Hence, they will show a higher SNR.

*reason 2:* When both TN and Pi cells are in the 'on' state, the TN cells let more light through, making for a bigger contrast between their dark and light state.

*6.2.3 Effect of yaw rotations.* As stated earlier, our system is resilient to roll rotations, but evaluating yaw rotations is important too. In all previous experiments, the LCs are facing the receiver, i.e. an approximate yaw angle of 0°. To test how the link performs with yaw offsets, we rotate the panel by -20, -10, 10, and 20 degrees. The BER of both TN and Pi cells are shown in Figure 10d. We can observe that the measurements are different for negative and positive offsets. This is because of the non-symmetrical arrangement of the cells. As the Pi cell transmitter is more compact and regular, it results in a more uniform increase in BER in both directions. Overall, we observe that the platform has some resilience to yaw offsets up to −10°, maintaining a BER below 1% for both types of cells at higher light intensities. However, this performance can be improved further with more compact and symmetric designs.

*6.2.4 Varying light intensity.* In Section 4.3, we stated that a retransmission of the preamble is not necessary if the light intensity changes. That is, the preamble gathered at light intensity X can be used to decode payloads obtained at light intensity Y. We test this property with both cells at 2 m. In each experiment, we transmit packets at three different light intensities: 260, 520, and 1000 Lux for TN cells, and 1.8, 2.2, and 3.6 kLux for Pi cells. Then the payloads are separated from the preambles, and the channel matrices obtained from each light intensity are used to decode all the payloads. The results are shown in Figure 11. For both types of cells, the BER remains below 0.3%. This implies that the preambles do not need to be re-transmitted when the intensity changes, which means that in the long term, Pi and TN cells could reach 8 kbps and 1.6 kbps, respectively.

The BER matrices also show that preambles with higher SNRs (1 kLux for TN cells and 3.6 kLux for Pi cells) lead to slightly better results, as the channel parameters are obtained in a more robust manner. As stated before, the resilience to changes in light intensity is obtained because: (i) at the preamble, channel matrices scale inherently to changes in intensity, and (ii) at the payload, our decoding process normalizes the signal with respect to its own *local* maxima.

## 6.3 Noise comparison

In Section 2.1, we stated that an advantage of a third polarizer is the reduction of noise from ambient light. In this part, we do two experiments to quantify this effect. The main setup in both experiments is a SISO configuration such as in Figure 4, and the voltage v(t) is kept constant. The difference between these experiments is that in the first one, we remove the polarizer, while we keep it in the second experiment. Figure 12b shows the AC histograms when the third polarizer is removed, and 12a shows the same histogram with the third polarizer. The comparison shows that this polarizer can reduce the spread of the noise. In addition to the histograms, We measured the AC Root Mean Squared (RMS) value to be 4.47 and 11.01 with and without the third polarizer, respectively. Therefore, the third polarizer can reduce the measured noise by less than 0.4×.

# 7 Related Work

We divide the related work into three main groups, and Table 3 summarizes the most related studies.

**Backscattering systems.** These are the most relevant systems to our work. Given that the SoA uses different types of LCs and ambient light intensities, to provide a fair comparison, our analysis focuses on the LC switching speed, modulation method, and data rate per number of LC cells.

*Simple modulation.* Retro-VLC uses the simplest modulation, OOK [13]. The authors state that the switching frequency of the LCs is 500 Hz, leading to 500 bps at a range of 1.5 m. The advantage of OOK is its simplicity, which we also use. Even though there is no LC characterization in [13], we can infer that our MIMO system

could allow Retro-VLC to achieve (at least[5]) 4 kbps using 9 of their original LCs[6].

*Advanced modulation.* Retro-VLC was followed by a series of notable contributions: PassiveVLC [23], RetroI2V [19], RetroTurbo [20] and RetroMUMIMO [21]. PassiveVLC uses *trend-based* modulation, achieving 1 kbps at 1 m using a single LC and PD. We infer that their LCs have a bandwidth of 250 Hz[7], so, we could reach at least 2 kbps using their LCs. RetroI2V achieves the same data rate but a distance of 80 m using 36 LCs, two PDs and a more powerful lamp. The paper does not provide a complete LC characterization, but they state that the toggle rate of their LC is 125 Hz. Thus, using 9 of those LCs, our system could deliver (at least) 1 kbps.

RetroTurbo and RetroMUMIMO are the most related studies. RetroTurbo has two components: superimposed modulation and QAM constellations. *Superimposed modulation* exploits LCs with fast charging phases. Using 8 LCs, the link achieves 2 kbps. And adding a 16-*QAM constellation* with 64 LCs and 4 PDs provides an extra ×4 improvement, enabling an impressive 8 kbps at 7 m. RetroMUMIMO uses the same LCs as Turbo-boosting, but exploits small manufacturing differences between LCs to create parallel channels. Grouping 4 LCs for a single channel, and running eight channels (32 LCs), the system achieves 500 bps per channel at 2 m. The LCs used by RetroTurbo and RetroMUMIMO are slightly slower than our LCs (refer to Table 3), which suggests that our system could reach 4.25 kbps using 9 of their LCs, improving the data rate by factors of 2 (RetroTurbo) and 4 (RetroMUMIMO).

*The above studies are notable and exploit polarization, but do not provide a comprehensive theoretical framework. The most related study left the invertibility of the channel matrix as an open challenge [21], which we solve with a novel system using three polarizers and a deep analysis of inexpensive color filters. Our analysis enables all these prior platforms (LCs) to achieve almost linear improvements with MIMO communication. But our framework could also be combined with trend-based modulation [23] or superimposed modulation [20] to achieve the best synergy between MIMO and advanced modulation schemes.*

**Transmissive systems.** Contrary to backscattering systems, which use retroreflectors to send light back, transmissive systems let the light pass through the LCs, and some of these studies have exploited color in different ways.

*Simple modulation.* LuxLink [3] uses frequency-shift-keying (FSK) to cope with the variability of sunlight. LuxLink achieves 1 kbps at 2 m using 4 LCs and 80 bps at 65 m using 2 LCs.

*Advanced modulation.* LCs can also modulate the color of ambient light. ChromaLux isolates a *single color channel* to obtain a faster-switching response, achieving 1.2 kbps at 50+ m with 6 LCs using sunlight [8]. SpectraLux modulates the color of the entire LC spectrum [7], enabling 1.5 kbps at 10 m using 4 LCs. None of these studies creates parallel channels inside the spectrum and their (de)modulation methods are complex. The most relevant study uses expensive (30 USD) dichroic filters to divide ambient light into *only* two channels [6]. The response of those filters is sharp, and hence, no model is required to tackle co-channel interference.

Compared to the above studies, we provide a MIMO approach and rely on simple filters, less than 1 USD, allowing simultaneous transmitters even with co-channel interference. The main advantage of the transmissive systems is that they exploit sunlight, while we exploit artificial (backscatter) light. However, advances in sunlight collectors [11] would allow our system to be used with sunlight as well.

Other studies using color modulation are Pixel [24] and Poli [4], but using a camera as a receiver. Due to the slow nature of LCs and cameras, Pixel achieves around 7 bps (using a single shutter) and Poli 72 bps (using three shutters). Using a PD instead of a camera, Pixelated-VLC [17] achieves 600 bps at 2 m. with three shutters Finally, some studies try to create MIMO links using LEDs as transmitters and cameras [12] and photodiodes [25] as receivers, but these studies have only been evaluated in simulations.

**Other systems.** Besides LCs, recent platforms are exploring digital-micro-mirror devices (DMDs) to modulate ambient light [22]. Contrary to LCs, DMDs have a higher switching speed, enabling data rates of 80 kbps. However, they have tiny surface areas (orders of $mm^2$), making it harder to design a system with multiple misaligned polarizers.

## 8 Discussion

In this section, we try to give a road map of potential improvements to the current design.

### 8.1 Size of the panels

In Section 6, we saw that at distances lower than 1 m the BER increased. This was due to the fact that some of the transmitting cells went out of the field-of-view (FoV) of the receivers. Had the transmitters been made small enough, this problem would not have appeared. To reduce the transmitters' size, a potential solution is to manufacture them similar to LCD monitors, where small LC pixels are made in repeating patterns. To make a MIMO system with 9 channels, we can manufacture 9 different pixels, which repeat across the whole panel of the transmitter. As a result, the 9 transmitters are always in the FoV by the receiver regardless of its distance.

### 8.2 Modulation

Regarding modulation, there are two aspects to discuss: the transmission of clock, and the type of modulation.

*8.2.1 Clock transmission.* we employed the simplest modulation scheme to avoid complication. While the transmitted clock occupies only 10% of the channel capacity, the throughput can be improved by using more advanced modulation schemes, such as FSK[3]. This way, the clock is recovered from preambles, and more bandwidth is assigned to data transmission.

*8.2.2 Type of modulation.* In some other works, advanced modulation schemes are used to compensate for the slow speed of liquid crystals. Some of these methods are orthogonal to that of this paper. In general, our MIMO sub-channels can use any modulation unless it depends on different polarizations or colors. Examples of such modulations are the trend-based [19] and FSK [3]. These two

[5]For this and future comparisons, we state *at least* because the decoding threshold of OOK could be reduced further to increase the data rate, but we would need the LC characterization to quantify the upper bound.
[6]To have a fair comparison, we assume using 8 data channels and one clock channel, similar to our implementation. Also, we assume a *long* payload, which eliminates the effect of the preamble duration.
[7]They use LCs that reach 125 bps using OOK and Manchester encoding.

papers only manipulate the intensity of light, therefore, they can be implemented in sub-channels of our MIMO link.

Some other papers use both intensity and polarization. For example, RetroTurbo [20], partly depends on intensity (their Delayed Superimposed Modulation), and partly on polarization differences. In this scenario, only the DSM can be used in a sub-channel of a MIMO link, potentially increasing the data rates by a factor of 3×.

## 8.3 Further evaluation

The evaluation done in Section 6 puts the theoretical model of this paper into test. However, despite proving the concept, these experiments lack in some aspects, e.g. dynamic scenarios, or links implementing only polarization or color. In the sections below, we set the stepping stones and present preliminary results to address these concerns.

**A design for a moving platform.** In order to test the multiplexed link in movement, we developed a robot carrying 3 LC cells. These cells constitute the transmitter of a MUMIMO channel using only polarization. A light source is pointed towards the robot. This light is modulated by the cells and reflects back towards the light source, since there are retroreflectors under each cell. Next, these 3 channels are sensed and demultiplexed using 3 photodiodes implemented close to the flashlight. The robot uses this link to transmit the data it collects via its sensors.

Besides showing a non-stationary link, we try to prove the following with the help of this initial prototype: a) Each modulation layer, polarization and color, can be used independently of the other to make a working link, and b) the misalignment of the transmitter and receiver does not affect the functionality of this link.

It is important to note this system's data rate, which is 300 bps, is still not competitive with the SoA, therefore, we present it as a motivation and a proof-of-concept for future work. Below we elaborate each of the aspects mentioned above.

*8.3.1 Using only polarization for multiplexing.* This prototype does not include any color filters. Therefore, it implements a *flat* mode of communication explained in Section 4. The BER and condition number of this link are measured at different distances. These results are shown in Figure 14. As expected, both parameters stay low except for short distances, which is explained by the transmitters going out of the FoV of all receivers. Additionally, comparison of figures 14a and 14b shows that condition numbers below 5 result in a BER of almost 0%.

*8.3.2 Misalignment of transmitter and receiver.* In this robot, the transmitting LC polarizers are placed to form 120°[8] with each other. When the robot moves, we expect the roll angle of the transmitters to change. To test the effect of this on the link, the robot is placed at a distance of 175 cm from its receiver, and its roll angle is changed from 0 to 175 degrees. The BER and condition number of this experiment are visible in Figure 15. Based on this, the roll angle does not affect the communication and the BER stays low.

In summary, this basic prototype is promising that 1) the link can be used with non-stationary targets, 2) we can implement channel multiplexing by using only polarization and leave out the color filters, and 3) the roll angle variations do not affect the communication.

In addition to all this effort, we still believe that it would be valuable to test this multiplexed communication a real automotive setup, such as the one done in [19]. In this case, The communication in scenario becomes challenging and requires more resilient modulation methods.

[8] in contrast to our system used in this paper, where the angles are at 0,45,90

**Table 3: SoA Summary: Comparison against platforms using multiple LCs at the transmitter. Some LCs work at a higher rate than their bandwidth. This is achieved by sacrificing SNR and switching LCs before reaching their steady states.**

| Work | LC bandwidth | Total Data rate | Data rate per LC | Type of (De)Mod. |
|---|---|---|---|---|
| **Our study** | 0.40 kHz | 6.8 kbps | 0.76 kbps | OOK |
| RetroMUMIMO | 0.25 kHz | 4.0 kbps | 0.125 kbps | ML-based |
| RetroTurbo | 0.25 kHz | 8.0 kbps | 0.125 kbps | DSM+QAM |
| SpectraLux | 0.40 kHz | 1.5 kbps | 0.375 kbps | ML-based |
| ChromaLux | 0.12 kHz | 1.2 kbps | 0.20 kbps | OOK |

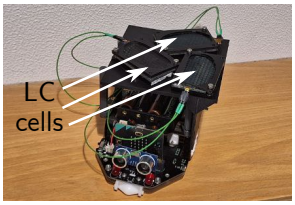


**Figure 13. A robot using 3 LCs to communicate**

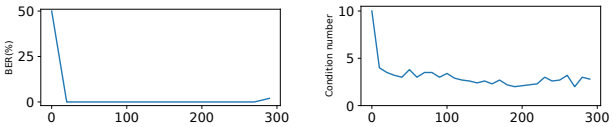


**(a) BER** **(b) Condition number**

**Figure 14. BER and condition number of robot link at different distances.**

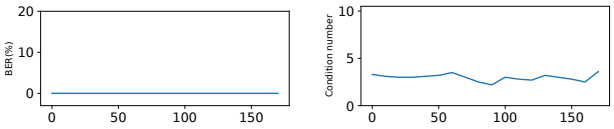


**(a) BER** **(b) Condition number**

**Figure 15. Effect of robot roll angles on BER and condition number.**

## 9 Conclusion

To increase the performance of passive-VLC, we looked into the powerful, but not well-explored method of MIMO. We revisited its theoretical framework and adapted it to liquid crystal (LC) cells. Our methods and prototypes show that the system's data rate increases almost linearly with the number of LCs, up to 9× the rate of a single cell. Our results show that for studies using multiple LCs at the transmitter, our method can improve the data rate per LC by factors between 2 and 6. Our work provides a stepping stone to

facilitate MIMO channels with passive-VLC and opens up multiple opportunities for further improvement.

## 10 Acknowledgements

This work is part of the *LuxSenz* project, a *TOP-Grant, Module 1, Physical Sciences* with project number 612.001.854, which is financed by the Dutch Research Council (NWO). We would also like to thank Justin de Ruiter for following up on the main research line of this paper and developing the robot platform mentioned in Section 8.

## References

[1] Color filter. https://www.amazon.com/Correction-Colored-Overlays-Transparency-Plastic/dp/B07WZM6TDT.

[2] M.Z. Afgani, H. Haas, H. Elgala, and D. Knipp. Visible light communication using ofdm. In *2nd International Conference on Testbeds and Research Infrastructures for the Development of Networks and Communities, 2006. TRIDENTCOM 2006.*, pages 6 pp.–134, 2006.

[3] Rens Bloom, Marco Zúñiga Zamalloa, and Chaitra Pai. Luxlink: creating a wireless link from ambient light. In *Proceedings of the 17th Conference on Embedded Networked Sensor Systems*, pages 166–178, 2019.

[4] Chun-Ling Chan, Hsin-Mu Tsai, and Kate Ching-Ju Lin. Poli: Long-range visible light communications using polarized light intensity modulation. In *Proceedings of the 15th Annual International Conference on Mobile Systems, Applications, and Services*, MobiSys '17, pages 109–120, New York, NY, USA, 2017. ACM.

[5] Robin Chataut and Robert Akl. Massive mimo systems for 5g and beyond networks—overview, recent trends, challenges, and future research direction. *Sensors*, 20(10):2753, 2020.

[6] Miguel Chavez, Talia Xu, and Marco Zuniga. Sol-fi: Enabling joint illumination and communication in enclosed areas with sunlight. In *Proceedings of the 23rd International Conference on Information Processing in Sensor Networks*, IPSN '24, New York, NY, USA, 2024. Association for Computing Machinery.

[7] Seyed Keyarash Ghiasi, Vivian Dsouza, Koen Langendoen, and Marco Zuniga. Spectralux: Towards exploiting the full spectrum with passive vlc. In *Proceedings of the 22nd International Conference on Information Processing in Sensor Networks*, IPSN '23, page 274–287, New York, NY, USA, 2023. Association for Computing Machinery.

[8] Seyed Keyarash Ghiasi, Marco A. Zúñiga Zamalloa, and Koen Langendoen. A principled design for passive light communication. In *Proceedings of the 27th Annual International Conference on Mobile Computing and Networking*, MobiCom '21, page 121–133, New York, NY, USA, 2021. Association for Computing Machinery.

[9] Chen He, Xun Chen, Zhen Jane Wang, and Weifeng Su. On the performance of mimo rfid backscattering channels, Nov 2012.

[10] Darko Ivanovich, Sam Powell, Roger Chamberlain, and Viktor Gruev. Polarization division multiplexing for optical data communications. page 50, 02 2018.

[11] Himawari Solar Lighting System Laforet Engineeing Co. JP. Lightning solution, 2022.

[12] Jai-Eun Kim, Ji-Won Kim, Youngil Park, and Ki-Doo Kim. Color-space-based visual-mimo for v2x communication. *Sensors*, 16(4), 2016.

[13] Jiangtao Li, *et al.* Retro-vlc: Enabling battery-free duplex visible light communication for mobile and iot applications. In *HotMobile*, 2015.

[14] Nanhuan Mi, Xiaoxue Zhang, Xin He, Jie Xiong, Mingjun Xiao, Xiang-Yang Li, and Panlong Yang. Cbma: Coded-backscatter multiple access. In *2019 IEEE 39th International Conference on Distributed Computing Systems (ICDCS)*, pages 799–809, 2019.

[15] GG Raleigh and John M Cioffi. Spatio-temporal coding for wireless communications. In *Proceedings of GLOBECOM'96. 1996 IEEE Global Telecommunications Conference*, volume 3, pages 1809–1814. IEEE, 1996.

[16] Neil A Rebolledo, Dmitri C Kyle, and Daniel P Phipps. Achromatic ferroelectric liquid crystal polarization rotator. In *Polarization: Measurement, Analysis, and Remote Sensing XIII*, volume 10655, pages 38–44. SPIE, 2018.

[17] Sihua Shao, Abdallah Khreishah, and Hany Elgala. Pixelated vlc-backscattering for self-charging indoor iot devices. *IEEE Photonics Technology Letters*, 29:177–180, 2017.

[18] Meng-Yu Tsai, Li-Chan Lai, and Jian-Jang Huang. 2-gbit/s data rate transmission for visible light communication using light-emitting diodes with photonic crystals. In *2020 Opto-Electronics and Communications Conference (OECC)*, pages 1–3, 2020.

[19] Purui Wang, Lilei Feng, Guojun Chen, Chenren Xu, Yue Wu, Kenuo Xu, Guobin Shen, Kuntai Du, Gang Huang, and Xuanzhe Liu. Renovating road signs for infrastructure-to-vehicle networking: a visible light backscatter communication and networking approach. In *Proceedings of the 26th Annual International Conference on Mobile Computing and Networking*, pages 1–13, 2020.

[20] Yue Wu, Purui Wang, Kenuo Xu, Lilei Feng, and Chenren Xu. Turboboosting visible light backscatter communication. In *Proceedings of the Annual conference of the ACM Special Interest Group on Data Communication on the applications, technologies, architectures, and protocols for computer communication*, pages 186–197, 2020.

[21] Kenuo Xu, Chen Gong, Bo Liang, Yue Wu, Boya Di, Lingyang Song, and Chenren Xu. Low-latency visible light backscatter networking with retromumimo. *Proceedings of the Twentieth ACM Conference on Embedded Networked Sensor Systems*, Nov 2022.

[22] Talia Xu, Miguel Chávez Tapia, and Marco Zúñiga. Exploiting digital Micro-Mirror devices for ambient light communication. In *19th USENIX Symposium on Networked Systems Design and Implementation (NSDI 22)*, pages 387–400, Renton, WA, April 2022. USENIX Association.

[23] Xieyang Xu, *et al.* PassiveVLC: Enabling practical visible light backscatter communication for battery-free iot applications. In *MobiCom*, pages 180–192, 2017.

[24] Zhice Yang, Zeyu Wang, Jiansong Zhang, Chenyu Huang, and Qian Zhang. Wearables can afford: Light-weight indoor positioning with visible light. In *Proceedings of the 13th Annual International Conference on Mobile Systems, Applications, and Services*, MobiSys '15, pages 317–330, New York, NY, USA, 2015. ACM.

[25] Yumeng Zhang, Yijun Zhu, Yan-Yu Zhang, Chao Wang, and Yu Mu. The structure determined of low ill-condition structure constraint spatial modulation for massive multi-color mimo-vlc. In *2019 IEEE/CIC International Conference on Communications in China (ICCC)*, pages 177–182, 2019.